Fiber-Optic Pyrometer for Very Localized Temperature Measurements in a Turning Process

A. Tapetado, J. Díaz-Álvarez, H. Miguélez, and C. Vázquez, *Senior Member, IEEE*

***Abstract*—A fiber-optic two-color pyrometer based on glass multimode fibers with 62.5 μm diameter and 0.275 numerical aperture is used for localized temperature measurements in turning processes. Operation wavelengths improve temperature measurement accuracy. The system is capable of measuring temperature in the range from 300 to 650 °C in a surface area below 0.16 mm^2. Numerical simulation of the calibration curves including manufacturer tolerances are reported, showing good agreement with the experimental results. Temperature evolution is performed in a lathe at different feed rates and cutting speeds at an Inconel 718 turning process, using a glass fiber-optic sensor embedded into a modified tool member. The results are used to in-process prevent premature failure of the components related to the fatigue and validate feed rates recommended by the tool manufacturer.**

***Index Terms*—Fiber-optics, turning process, temperature measurement, two-color pyrometer, demultiplexer, wavelength division multiplexing, embedded glass fiber, Inconel 718.**

I. Introduction

MANUFACTURING critical components for high responsibility application such as the aircraft engine components commonly based on Ni superalloys requires ensuring the surface integrity of the piece. The physical and chemical phenomena, which take place during the machining process, could lead to workpiece surface oxidation, superficial and internal residual stresses, and precipitations of different alloys elements [1]. These phenomena are strongly related to the temperature reached at the workpiece during the machining process, thus it is important to measure this temperature.

Machining induced residual stresses caused by plastic deformation, thermal effects, microstructure changes and phase transformation are important indicators of surface integrity when machining superalloys.

Although the mechanisms involved are not completely clear it is commonly accepted the opposite effect of plastic deformation inducing compressive stress at the surface while thermal effects cause tensile stresses [2]–[4]. Tensile stresses are related to a decreased fatigue life of the components [5]. Both effects are coupled and also interact with phase transformation causing volumetric changes. The effect of temperature is more significant when machining super alloys such as Inconel 718 due to their heat resistance and poor thermal conductivity.

Temperature also affects Ni alloys machinability through the thermal softening of the workpiece material. This effect has motivated the external application of a laser heat source in order to diminish cutting forces and improve tool life when machining Inconel 718 [4].

Both surface integrity and tool life are strongly influenced by temperature level so localized accurate temperature measurements during the process are crucial.

The measurement of high temperatures has been reported using thermocouples [6]–[9], infrared (IR) cameras [10] and fiber Bragg gratings (FBGs) [11], [12]. The majority of the thermocouples and IR cameras measure temperature on the rake [6], [7], [9] and flank face [6], [7], [10] of the cutting tool. But the difficulty of installation between the flank face and the workpiece surface make them unsuitable for temperature measurements. In addition, FBGs are also contact sensors that may have the disadvantage of its fragility and difficulty of installation close to the measuring point. Only few proposals [8] provide a good solution for temperature measurements on the workpiece surface but with the difficulty of installing embedded sensors in the cutting tool.

Two-color fiber-optic pyrometer is a possible solution to overcome these constraints. It uses the ratio of optical powers at two spectral bands to implement a self-referencing technique in order to avoid the emissivity dependence of temperature as reported by B. Müller *et al.* [13] and A. Tapetado *et al.* [14], among others [15], [16]. The use of optical fibers allows viewing localized areas with a spatial resolution limited by the numerical aperture and dimensions of the fiber. In previous works, several authors propose measuring temperatures around 300 °C but using large fiber diameters [15]–[17], increasing the measuring area and thus, reducing spatial resolution. Neither works justifies their measurements with mechanical approximations.

Manuscript received June 5, 2016; revised August 16, 2016; accepted November 7, 2016. Date of publication November 29, 2016; date of current version December 9, 2016. This work was supported in part by the Ministerio de Economía, Industria y Competitividad of Spain under Grant TEC2015-63826-C3-2-R (GREENFIBER) and Grant DPI2014-56137-C2-2-R, FEDER and in part by the Comunidad de Madrid under program S2013/MIT-2790 (SINFOTON-CM). A. Tapetado also acknowledges support from Fondo Social Europeo.

A. Tapetado and C. Vázquez are with the Displays and Photonics Applications Group, Electronics Technology Department, Carlos III University of Madrid, Madrid 28911, Spain (e-mail: atapetad@ing.uc3m.es; cvazquez@ing.uc3m.es).

J. Díaz-Álvarez is with the Aerospace Engineering Department, Carlos III University of Madrid, Madrid 28911, Spain (e-mail: jodiaz@ing.uc3m.es).

H. Miguélez is with the Mechanical Engineering Department, Carlos III University of Madrid, Madrid 28911, Spain (e-mail: mhmiguel@ing.uc3m.es).

Color versions of one or more of the figures in this paper are available online at http://ieeexplore.ieee.org.

Digital Object Identifier 10.1109/JSTQE.2016.2627553

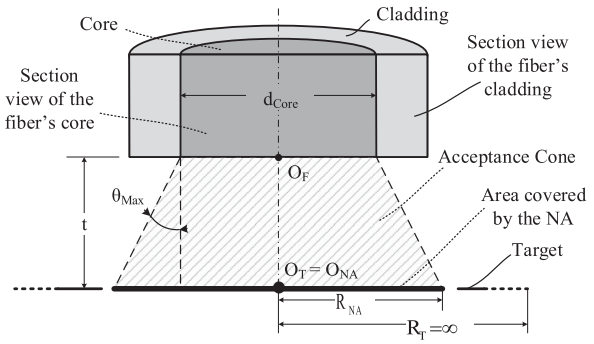

Fig. 1. Schematic of the optical fiber pyrometer measurement surface area.

In this work, we use an optimized fiber-optic two-color pyrometer [14], [18] to measure the temperature evolution of a workpiece of Inconel 718 at different cutting conditions. Commercial off-the shelf optoelectronics and fiber-optic components are used. The temperature evolution is performed in a lathe at different feed rates and cutting speeds. The fiber-optic sensor is embedded into a modified tool member which permits a highly localized temperature measurement on the workpiece surface. The results are justified and used to prevent the premature failure of the component related to the fatigue.

II. Principle of Operation

Every physical body at a specific temperature (*T*) emits electromagnetic radiation in all directions. The quantity of this radiation is called spectral radiance (*L*) and is described by Planck's law versus temperature and wavelength (λ) as [19]:

$$L(\lambda, T) = \frac{C_1 \cdot \varepsilon(\lambda, T)}{\lambda^5 \cdot \left(e^{\frac{C_2}{\lambda \cdot T}} - 1\right)} \tag{1}$$

where ε is the emissivity of the measured object, C_1 and C_2 are the Planck's radiation constants, whose values are $1.19{\cdot}10^8$ W·Sr^{-1}·μm^4·m^{-2} and $1.44{\cdot}10^4$ μm·K, respectively.

A two-color fiber-optic pyrometer gathers radiation from a body over a wide spectral region but divides the radiation into two wavelength bands using a filter. The filtering channels are linked to photodetectors (PDs) for measuring the optical power at different wavelength bands.

Only rays inside the acceptance cone of the optical fiber are collected and transmitted, see Fig. 1. This acceptance angle (θ_{Max}) depends on the optical fiber numerical aperture (NA).

The influence of the setting location of the fiber on the spectral radiance accepted and transmitted by the fiber is analyzed in [14], [20]. The fiber end is vertically placed above the target surface at a distance (*t*), see Fig. 1. We assume a target radius (R_T) much greater than the spot radius (R_{NA}) projected by the fiber NA. Therefore, the optical power measured by the pyrometer can be expressed by [14]:

$$P_D(T, \lambda) = \int_{\lambda_A}^{\lambda_B} \frac{C_1 \cdot IL(\lambda) \cdot \alpha(\lambda) \cdot \varepsilon(\lambda, T)}{\lambda^5 \cdot \left(e^{\frac{C_2}{\lambda \cdot T}} - 1\right)} \cdot \kappa(\lambda) \cdot d\lambda \tag{2}$$

where $\kappa(\lambda)$ is the coupling loss given by [20]:

$$\kappa(\lambda) = \frac{\pi^2 \cdot d_{\mathrm{Core}}^2}{8} \cdot \left[1 - \cos\left(2 \cdot \theta_{\mathrm{Max}}(\lambda)\right)\right] \tag{3}$$

being λ_A and λ_B the shortest and the longest wavelengths within the wavelength band provided by the optical filter, *IL* the insertion loss of the filter, α the fiber attenuation coefficient, and d_{Core} the fiber core diameter.

If a two-color pyrometer working at single wavelengths channels λ_1 and λ_2 is considered, the measured ratio temperature (T_R) is given by [14]:

$$T_R = \left[\frac{1}{T} + \frac{\ln(\varepsilon_r \cdot \delta_r)}{C_2 \cdot \left(\frac{(-4)\cdot\Delta\lambda}{4\cdot\lambda_c^2 - \Delta\lambda^2}\right)}\right]^{-1} \tag{4}$$

where *T* is the true temperature, λ_c and $\Delta\lambda$ are the average central wavelength and the wavelength spacing of the single wavelength channels, respectively, δ_r is the pyrometer loss ratio, and ε_r is the surface emissivity ratio. And the relative temperature error (E_T) is given by [13]:

$$E_T = \frac{(T_R - T) \cdot 100}{T} \quad [\%] \tag{5}$$

As appointed by Tapetado *et al.* in [14], the pyrometer temperature error (E_T) is not only dependent on the selected wavelength bands but also on the spectral characteristics of the devices employed in the pyrometer set-up. A good selection of the pyrometer wavelength bands allows compensating the losses of each device, to minimize the pyrometer temperature error and to enhance the minimum measurable temperature. The pyrometer described in this work uses low-loss optical components designed for telecommunication purposes in order to achieve a temperature error reduction without thermal cooling and high spatial resolution. According to these aspects, the optimized wavelength bands are chosen to be at 1.3 and 1.55 μm [14].

III. Pyrometer Design

The sensor is made of standard graded-index glass optical fiber OM1 with 62.5/125 core and cladding diameters in microns. This fiber is capable of measuring highly localized temperatures measurements without using lenses. Using a fiber numerical aperture of 0.275, the measured spot diameter is 0.16 mm, very localized in comparison to previous designs covering in the same conditions a spot diameter of 0.48 mm [17]. The fiber length is fixed at 0.5 m to reduce the impact of fiber-optic attenuation on the temperature measurements. A low insertion loss WDM fiber-optic filter is arranged to spatially split the radiation collected by the optical fiber into two spectral bands centered at 1.3 and 1.55 μm, respectively. Finally, a dual InGaAs PD with uniform responsivity values at both wavelengths bands is used. The maximum optical power measurable by both PDs is 10 mW. The schematic of the pyrometer and the experimental set-up are shown in Fig. 2.

IV. Calibration

The two-color fiber-optic pyrometer is calibrated using a dry block calibrator and a blackbody kit, see Fig. 3.(a). The control unit ensures a maximum temperature stability and uncertainty

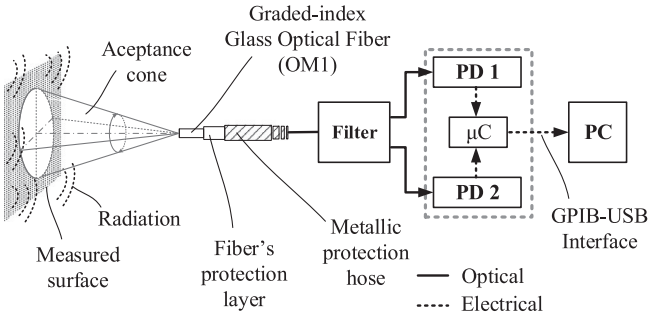

Fig. 2. Schematic of the pyrometer and the experimental set-up.

Fig. 3. (a) Photograph of the dry block calibrator and the blackbody on top of it. (b) Photograph of the metallic holder used to place the optical fiber on the blackbody.

of ±0.03 and ±0.17 °C, respectively, in the range from 50 to 650 °C. The emissivity of the blackbody is greater than 0.99.

As pointed out by Tapetado et. al. in [21], temperature measure is insensitive to the fiber position if the target surface is larger than the spot projected by the fiber NA on the measuring surface. The fiber sensor is fixed at a distance of 0.3 mm from the blackbody using a calibrated metallic holder, as shown in Fig. 3(b). Using this distance and the fiber NA, the spot area is 0.043 mm^2. Thus, considering a blackbody surface emitting area of ∼700 mm^2, the temperature measure at around this distance is insensitive to the fiber position.

To facilitate the fiber set-up and to avoid the fiber breakage during the positioning of the fiber in the metallic holder, a high temperature protection hose made of heat-treatable stainless steel is used to give more rigidity to the fiber end. The protection hose has an external and internal diameter of 1 and 0.14 mm, respectively.

The radiant flux emitted by the blackbody has been characterized at 1.3 and 1.55 μm spectral bands, meanwhile the temperature of the blackbody surface changes from 300 to 650 °C at 10 °C intervals. The sample rate and the number of samples at each temperature and wavelength are fixed at 1 kHz and 10 S, respectively. A time interval of 45 min between each temperature measurement is set to provide the stability of the measurements. The average of the measured optical power ratio at both spectral bands for each temperature is calculated from the mean of the samples. The optical power measured by the fiber-optic pyrometer at a temperature of 300 °C is 9.5 and 8.6 pW for a filtering channel of 1.3 and 1.55 μm, respectively. Thus, these values are higher than the photodetector power accuracy of 1.1

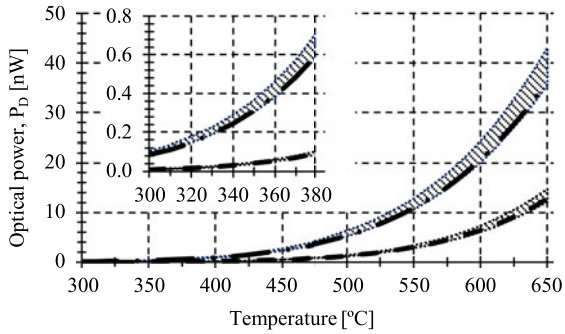

Fig. 4. Output power variations versus temperature for the theoretical (filled areas) and experimental (dashed lines) calibration curves at different wavelength bands: (– –) 1.3 μm, (– · –) 1.55 μm. Inset included for temperature range 300–380 °C.

and 3.4 pW, respectively. Therefore, the proposed fiber-optic pyrometer is capable of measuring temperatures above 300 °C. On the other hand, the maximum temperature is limited by the melting point of the optical fiber used in the experimental set-up. For this application, a bare silica fiber with a melting point of ∼1600 °C is used. Evaluating (2) at a temperature of 1600 °C, it is theoretically estimated that a maximum optical power of 8 and 6 μW should measure by both PDs of both pyrometer channels, respectively. Therefore, these values are lower than the maximum optical power measurable by both PDs.

Using (2) and (3) the optical power measured by each PD is simulated from 300 to 650 °C at 10 °C intervals. Experimental results and simulations are shown on Fig. 4. At the first wavelength band, the longest and shorter wavelength limits are 1.43 and 0.8 μm, respectively. On the other hand, the second filtering channel contains signals from 1.38 to 1.7 μm. The wavelength range of the InGaAs responsivity curve delimits wavelength bands. Filter insertion losses of 0.21 and 0.06 dB at 1.3 and 1.55 μm are considered. The emissivity of a blackbody is used in the simulations. The responsivity of an InGaAs photodetector is 0.89 and 0.99 A/W at 1.3 and 1.55 μm, respectively. Finally, fiber attenuation at 1.3 and 1.55 μm is 0.58 and 0.26 dB/km, respectively. Applying (4) and (5), the pyrometer temperature error obtained considering all wavelength dependence loss ratio is 5.5% for an emissivity ratio of 1 and a temperature of 500 °C.

The measured output optical power is strongly conditioned by the optical fiber core diameter. The optical fiber is made of glass and manufactured using a drawing tower that fixed the core and cladding diameter. The smaller fiber diameter the more difficult is the drawing process. The optical fiber used in this experiment has a tolerance in the nominal core diameter of ±3 μm. Output optical power at each wavelength band is simulated varying the nominal core diameter, see Fig. 4.

From Fig. 4 is clear that the experimental calibration curves are within the diameter tolerance given by the manufacturer. The diameter that provides the closest agreement between the theoretical and experimental curves is 61.4 μm.

V. Experimental Results

A. Tool Member and Fiber Position

The amount of heat generated in a turning process mainly depends on the workpiece material, cutting speed, feed rate

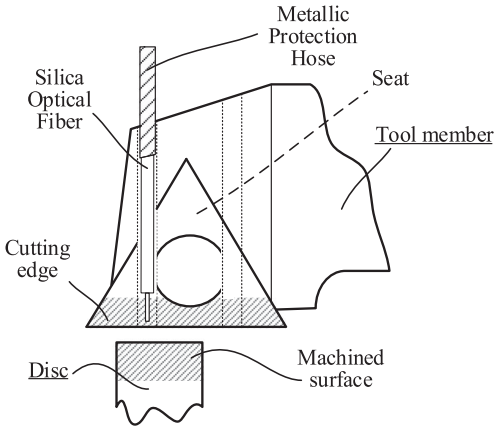

Fig. 5. Top view of the tool member with the optical fiber during the orthogonal machining process.

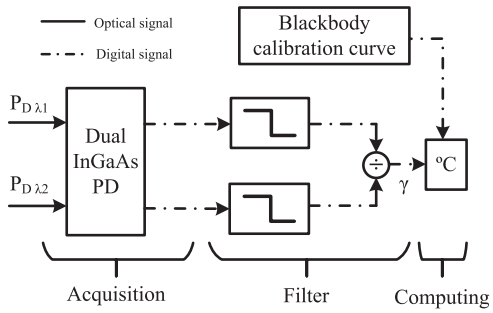

Fig. 6. Block diagram of the computer software used to acquire and post-process all signals.

and depth of cut, among others. During a cutting process, heat is continually removed from the cutting edge toward to the chip-tool and the tool-workpiece interfaces. It has been found convenient to locate the measuring point at the fresh machined surface in order to evaluate the workpiece surface temperature and thus to control the mechanical and chemical properties of the final workpiece [22].

The temperature of a heated surface of the workpiece is measured by viewing the machining surface directly with an optical fiber and transmitting the radiant energy emitted from the heated surface to the two-color fiber-optic pyrometer, see Fig. 5. The hot spot is viewed directly by means of the small diameter hole formed into the tool member through tool holder and seat. The fiber hole within seat has a diameter of 1.3 mm. A high temperature protection hose made of stainless steel avoids the fiber breakage during the cutting process and allows keeping the right fiber position in the tool member giving more rigidity to the fiber end. The distance between the cutting edge and the fiber hole is 4 mm. This distance is limited by the capability of the drilling process to machine small diameter holes in hard materials such as carbide tool inserts. The fiber is placed at a distance of 0.3 mm from the machined surface and the positioning method guaranteed a positioning tolerance of ± 0.05 mm. Every time the material is removed, temperature at the surface is measured, not after multiple turns to reach steady conditions as in [14].

B. Virtual Processing System

A computer software is designed to acquire and post-process the signals for the two wavelength bands. There are three stages: acquisition, filtering and computing, as shown in Fig. 6.

The first stage uses a communication control unit to configure and start the acquisition process of the dual InGaAs PD. The acquisition rate and the number of samples per channel are set to 1 kS/s and 10,000 samples, respectively. These values are selected to assure a minimum acquisition time of 10 s. The synchronism mode in the dual PD is activated in order to acquire samples at the same time. The second stage uses a digital low-pass filter to eliminate noise from all acquired signals. The designed filter uses a fifth order Finite Impulse Response topology. The pass and stop frequencies are fixed at 20 and 35 Hz. Finally, a computing stage is implemented to internally calculate the estimated temperature. This stage calculates the output power ratio of both filtered signals and then using the calibration curve of the blackbody, estimates the cutting temperature.

C. Temperature Measuring Conditions

The machining experiments are conducted for continuous turning under two-dimensional orthogonal cutting conditions. A heat-treatable Inconel 718 bar with a diameter of 120 mm is used to manufacture the workpieces used in the experimental set-up. A circular cut plate with a thickness of 2 mm is cut from the bar using a wire electrical discharge machining. Afterwards, the workpiece is located on a mandrel with a feed motion applied radially toward the axis of the cut plate. The modified tool member is used to hold an uncoated carbide tool insert (TCMW 16 T3 08 H13A) which has a rake and clearance angle of 0 and 7 °, respectively. The maximum feed rate (f) and cutting speed (V_c) recommended by the manufacturer is 5.60 mm and 80 m/min, respectively. On the other hand, the minimum and maximum feed rates are 0.08 and 0.53 mm/r, respectively.

Using the computer software and the pyrometer set-up, temperature evolution on the workpiece surface is performed with three values of the feed rate: 0.05, 0.1 and 0.15 mm/r. Feed rates of 0.1 and 0.15 mm/r are in the range recommended by the tool manufacturer for this tool geometry. For each feed rate, the cutting velocity is changed at 60, 90, 120, 240 m/min. In all these measurements, the depth of cut is fixed at 2 mm. No cutting fluids are used in the experiments. The cutting process takes less than 2s, thus the tool geometry is not affected by wear on the turning process.

Fig. 7 shows temperature evolution on the workpiece surface for a feed rate, cutting velocity and depth of cut of 0.15 mm, 90 m/min and 2 mm, respectively.

Two different regions are observed. The first region is a transient regime and occurs when the cutting tool starts to remove material form the workpiece. The radiation emitted by the workpiece is not great enough to be measured by the PDs. The PD noise is 3.4 and 1.1 pW for a wavelength of 1.3 and 1.55 μm, respectively. After 0.45 s from the beginning of the cutting process, cutting and thrust forces reach a stationary regime. The

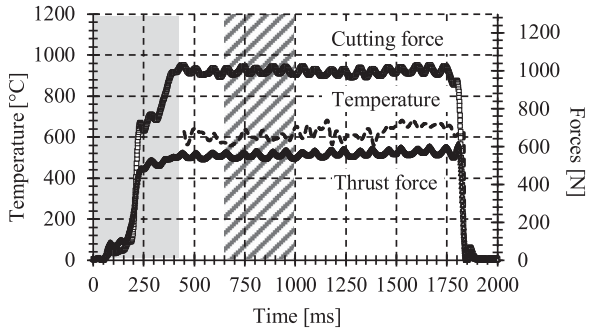

Fig. 7. Temperature measurements (discontinuous line), and cutting (square dots) and thrust (triangle dots) force evolution when machining Inconel 718 with a carbide cutting tool: $V_c = 90$ m/ min, d = 2 mm, f = 0.15 mm.

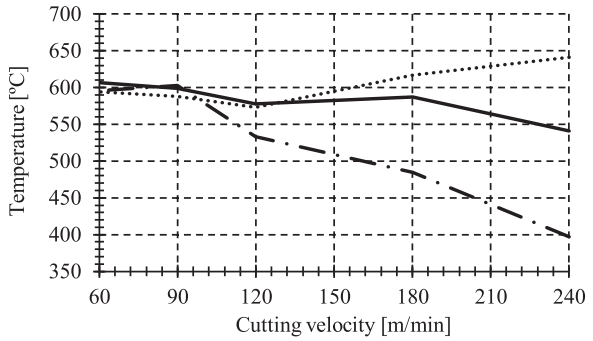

Fig. 8. Temperature of the workpiece as functions of cutting speed for different feed rates: $(- \cdot -)\, f = 0.15$ mm/ r, $(--)\, f = 0.1$ mm/ r, $(\cdot \cdot \cdot)\, f = 0.05$ mm/ r.

measured temperature where the cutting and thrust forces are completely stable is considered, as shown in striped region in Fig. 7. From this region, it is clear that the temperature of the cutting process is around 600 °C.

D. Discussion

The evolution of the temperature at the machined surface vs the cutting velocity for three different feeds is shown in Fig. 8. There is a clear decreasing trend for the temperature reached at the workpiece surface with respect to the cutting speed for feeds 0.1 and 0.15 mm/r, whereas the opposite trend is found for a feed rate of 0.05 mm/r.

The unexpected values found for the smallest value of the feed can be due to relative values of cutting edge radius (25 μm) and feed (0.05 mm), causing the tool to cut with an effective negative rake angle (in fact this value of feed is not recommended by the tool manufacturer, and it is only used to check the performance of the measuring system). Cutting with large cutting edge radius and low values of feed is related to elevated levels of deformation and temperature at the machined surface.

The Péclet number (dimensionless number extensively used in heat transfer problems) which relates the thermal energy extracted by the chip to that conducted to the workpiece [23] is used to analyze the results. The Péclet number has the following

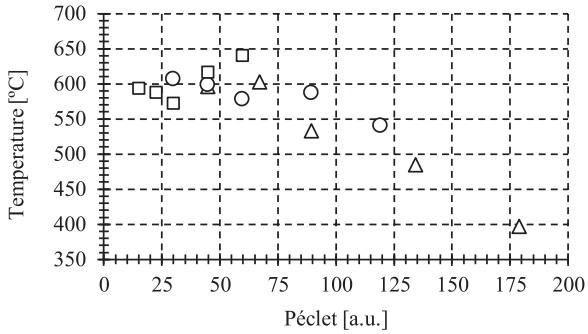

Fig. 9. Temperature of the workpiece as function of Péclet number for different feed rates: (Δ) f = 0.15 mm/ r, $(\circ)$ f = 0.1 mm/ r, $(\square)$ f = 0.05 mm/ r.

expression [23]:

$$P_e = \frac{v \cdot t_1}{w_w} \tag{6}$$

when applied to turning v is the cutting speed, t_1 is the undeformed chip thickness and w_w is the thermal diffusivity of the workpiece material.

Our results agree with previous studies that show that for large Péclet number more heat goes to the chip, and therefore less goes to the workpiece, increasing the fatigue life of the components (see Fig. 9) [24].

VI. Conclusions

Temperature measurement in areas located on the machined surface and close to the cutting zone is an important challenge in order to prevent premature failure in machining aerospace components. A two-color fiber-optic pyrometer with high spatial resolution has successfully been used to characterize the workpiece temperature in a high-speed turning process. The pyrometer uses conventional multimode optical fibers and wavelength bands used in local area networks. Simulations show that the experimental calibration curves are within the diameter tolerance given by the optical fiber manufacturer.

A high-accuracy fiber positioning method together with a standard graded-index glass optical fiber, allows to measure a very localized spot diameter of 0.16 mm.

Temperature on a workpiece of Inconel 718 are measured using the pyrometer set-up at different cutting speeds and feed rates, similar to those imposed during current industrial operations. Analytical model based on the Péclet number is used to estimate the temperature tendency at different cutting conditions. The results show that for large Péclet number more heat goes to the chip, and therefore less heat goes to the workpiece, reducing the surface temperature and thus, the fatigue life of the components. These results demonstrate that the pyrometer can be used to prevent the premature failure of the components related with the fatigue.

Acknowledgment

The authors would like to thank Eng. Ernesto Garcia Ares for his collaboration in developing the positioning stage.

REFERENCES

[1] A. Javidi, U. Rieger, and W. Eichlseder, "The effect of machining on the surface integrity and fatigue life," *Int. J. Fatigue*, vol. 30, nos. 10/11, pp. 2050–2055, Oct. 2008.

[2] M. H. Miguélez, R. Zaera, A. Molinari, R. Cheriguene, and A. Rusinek, "Residual stresses in orthogonal cutting of metals: The effect of thermomechanical coupling parameters and of friction," *J. Therm. Stresses*, vol. 32, no. 3, pp. 269–289, Feb. 2009.

[3] J. Díaz-Álvarez, J. L. Cantero, H. Miguélez, and X. Soldani, "Numerical analysis of thermomechanical phenomena influencing tool wear in finishing turning of Inconel 718," *Int. J. Mech. Sci.*, vol. 82, pp. 161–169, 2014.

[4] J. L. Cantero, J. Díaz-Álvarez, M. H. Miguélez, and N. C. Marín, "Analysis of tool wear patterns in finishing turning of Inconel 718," *Wear*, vol. 297, nos. 1/2, pp. 885–894, Jan. 2013.

[5] R. Avilés, J. Albizuri, A. Rodríguez, and L. N. López de Lacalle, "On the fatigue strength of ball burnished mechanical elements," in *Proc. Second Conf. MeTrApp*, Bilbao, Spain, 2014, pp. 365–373.

[6] T. Kitagawa, A. Kubo, and K. Maekawa, "Temperature and wear of cutting tools in high-speed machining of Inconel 718 and Ti-6Al-6V-2Sn," *Wear*, vol. 202, no. 2, pp. 142–148, Jan. 1997.

[7] N. Narutaki, Y. Yamane, K. Hayashi, T. Kitagawa, and K. Uehara, "High-speed machining of Inconel 718 with ceramic tools," *CIRP Ann. Manuf. Technol.*, vol. 42, no. 1, pp. 103–106, Jan. 1993.

[8] G. Le Coz and D. Dudzinski, "Temperature variation in the workpiece and in the cutting tool when dry milling Inconel 718," *Int. J. Adv. Manuf. Technol.*, vol. 74, no. 5, pp. 1133–1139, 2014.

[9] R. T. Coelho, L. R. Silva, A. Braghini, and A. A. Bezerra, "Some effects of cutting edge preparation and geometric modifications when turning Inconel 718 at high cutting speeds," *J. Mater. Process. Technol.*, vol. 148, no. 1, pp. 147–153, May 2004.

[10] C. Dinc, I. Lazoglu, and A. Serpenguzel, "Analysis of thermal fields in orthogonal machining with infrared imaging," *J. Mater. Process. Technol.*, vol. 198, nos. 1/3, pp. 147–154, Mar. 2008.

[11] J. He *et al.*, "Negative-index gratings formed by femtosecond laser overexposure and thermal regeneration," *Sci. Rep.*, vol. 6, Mar. 2016, Art. no. 23379.

[12] C. Zhang, Y. Yang, C. Wang, C. Liao, and Y. Wang, "Femtosecond-laser-inscribed sampled fiber Bragg grating with ultrahigh thermal stability," *Opt. Express*, vol. 24, no. 4, Feb. 2016, Art. no. 3981.

[13] B. Müller and U. Renz, "Development of a fast fiber-optic two-color pyrometer for the temperature measurement of surfaces with varying emissivities," *Rev. Sci. Instrum.*, vol. 72, no. 8, 2001, Art. no. 3366.

[14] A. Tapetado, J. Diaz-Alvarez, M. H. Miguelez, and C. Vázquez, "Two-color pyrometer for process temperature measurement during machining," *J. Lightw. Technol.*, vol. 34, no. 4, pp. 1380–1386, Feb. 2016.

[15] J. Thevenet, M. Siroux, and B. Desmet, "Measurements of brake disc surface temperature and emissivity by two-color pyrometry," *Appl. Therm. Eng.*, vol. 30, nos. 6/7, pp. 753–759, May 2010.

[16] F. J. Madruga, D. A. F. Fernandez, and J. M. Lopez-Higuera, "Error estimation in a fiber-optic dual waveband ratio pyrometer," *IEEE Sens. J.*, vol. 4, no. 3, pp. 288–293, Jun. 2004.

[17] B. Müller, U. Renz, S. Hoppe, and F. Klocke, "Radiation thermometry at a high-speed turning process," *J. Manuf. Sci. Eng.*, vol. 126, no. 3, pp. 488–495, 2004.

[18] C. Vázquez, A. Tapetado, H. Miguélez, and J. Díaz-Álvarez, "Pirómetro de Fibra Óptica a Dos Colores," Spanish Patent Appl. P201530546/5209ES, 2015.

[19] R. G. Driggers, C. Hoffman, and R. Driggers, *Encyclopedia of Optical Engineering*, 1st ed. Boca Raton, FL, USA: CRC Press, 2003.

[20] T. Ueda, A. Hosokawa, and A. Yamamoto, "Studies on temperature of abrasive grains in grinding—Application of infrared radiation pyrometer," *J. Eng. Ind.*, vol. 107, no. 2, pp. 127–133, 1985.

[21] A. Tapetado, E. García, J. Díaz-Álvarez, M. H. Miguélez, and C. Vázquez, "Optical-fiber pyrometer positioning accuracy analysis," *Proc. SPIE*, vol. 9916, 2016, Art. no. 99160F.

[22] R. Komanduri and Z. Hou, "A review of the experimental techniques for the measurement of heat and temperatures generated in some manufacturing processes and tribology," *Tribol. Int.*, vol. 34, no. 10, pp. 653–682, Oct. 2001.

[23] J. P. Davim, *Traditional Machining Processes*. Berlin, Germany: Springer, 2015.

[24] T. Childs, *Metal Machining: Theory and Applications*, London, U.K.: Butterworth-Heinemann, 2000.

A. Tapetado received the M.Sc. degree in industrial electronics engineering from the University of Castilla-La Mancha, Ciudad Real, Spain, in 2009, and the Ph.D. degree in electrical engineering, electronics, and automation from Polytechnic School, Carlos III University of Madrid, Madrid, Spain, in 2015. He was a Visiting Student at Aston Institute of Photonics Technologies, Aston University, Birmingham, U.K., in 2012, and at the Research Laboratory of Electronics, in 2013, working on polymer optical fiber Bragg gratings and silicon photonics, respectively. He is currently a Doctoral Researcher in the Department of Electronics Technology, Carlos III University of Madrid. His research interests include polymer and silica fiber optics sensors, sensor networks, integrated optics, and broadband access networks. He is a member of the Displays and Photonic Application Group.

J. Díaz-Álvarez received the degree in Industrial engineering in 2006 and the Ph.D. degree in 2013. He is an Assistant Professor in the Department of Bioengineering and Aerospace Engineering, Carlos III University of Madrid, Madrid, Spain, where he developed his research work focusing on the manufacturing processes. Between 2006 and 2009, he worked for several multinational companies devoted to the production of different goods.

H. Miguélez is a Full Professor at the Department of Mechanical Engineering, Carlos III University of Madrid, Madrid, Spain, where she received the Ph.D. degree and a degree in aeronautical engineering from the Polytechnic University of Madrid, Spain. She is the Head of the Manufacturing Technologies and Components Design Group. Her research interests include machining tools and techniques, and modelling of machining processes and defects.

C. Vázquez (M'99–SM'05) received the M.Sc. degree in physics (electronics) in 1991 from the Complutense University of Madrid, Madrid, Spain, and the Ph.D. degree in photonics from the Telecommunications Engineering School, Polytechnic University of Madrid, Madrid, Spain, in 1995. She received a fellowship at TELECOM, Denmark, in 1991, working on erbium-doped fiber amplifiers. From 1992 to October 1995, she worked at the Optoelectronics Division of Telefnica Investigacin y Desarrollo. She was involved in III–V integrated optics devices characterization, design, and fabrication. In October 1995, she joined Carlos III University of Madrid, Madrid, Spain, where she is currently a Full Professor in the Department of Electronics Technology and the Head of the Displays and Photonic Applications Group. She was a Visiting Scientist at the Research Laboratory of Electronics, Massachusetts Institute of Technology from August 2012 to July 2013, working on silicon photonics. She was also the Head of the Department for 3 years and the Vice-Chancellor for four years. Her research interests include integrated optics, optical communications and instrumentation including, plastic optical fibers, broadband access networks and monitoring techniques, RoF systems, filters, switches, fiber optic sensors, and WDM networks. She has published more than 200 scientific publications and is the holder of five patents. She has participated in different European projects and networks in the ESPRIT, RACE and IST framework programs such as PLANET, OMAN, HEMIND, SAMPA, EPhoton/One+, BONE (*Building the Future Optical Network in Europe*), etc., and has led several national researching projects and consortium such as SINFOTON-CM. She is a Fellow of the SPIE.